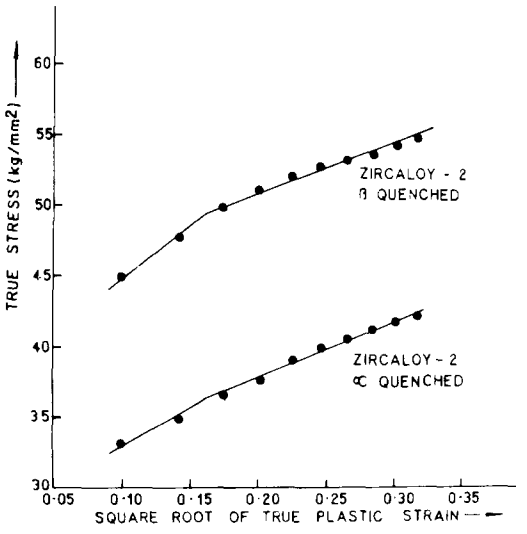

Figure 6 True stress versus square root of true plastic strain plots for zircaloy-2.

localized flow of some regions of high stress concentration. Beyond the transition at $\epsilon_p \simeq 3\%$, the work hardening could be expected to have been governed mainly by the short range interaction of the gliding dislocations with the geometrically necessary ones.

For zircaloy-2, the σ versus $\epsilon_p^{1/2}$ plots consisted of two linear segments, the transition occurring again at $\epsilon_p \simeq 3\%$ (Fig. 6). The flow behaviour was similar to that of Zr–1.5% Sn in that the martensitic and the non-martensitic structures were associated with nearly the same work hardening rates at strains exceeding 3%. It was likely that in this case the flow was controlled by the distribution of the θ precipitates [8] formed during quenching.

References

1. J. W. CHRISTIAN, "Strengthening Methods in Crystals" (Elsevier, London, 1971) p. 261.
2. H. WARLIMONT and L. DELAEY, *Prog. Mater. Sci.* 18 (1974) 117.
3. C. D. WILLIAMS and R. W. GILBERT, *Trans. Jap. Inst. Metals* 9 (Supplement) (1968) 625.
4. S. BANERJEE, Ph.D. Thesis, Indian Institute of Technology, Kharagpur (1973).
5. M. HANSEN, "Constitution of Binary Alloys", (McGraw–Hill, New York, 1958).
6. M. F. ASHBY, "Strengthening Methods in Crystals" (Elsevier, London, 1971) p. 137.
7. A. K. SINHA, *Prog. Mater. Sci.* 15 (1972) 93.
8. D. L. DOUGLASS, *J. Nucl. Mater.* 9 (1963) 252.

Received 9 December 1977
and accepted 19 January 1978

V. RAMAN
P. MUKHOPADHYAY
Metallurgy Division,
Bhabha Atomic Research Centre,
Trombay, Bombay 400 085, India

Azimuthal rotation in epitaxial CdSe/Ge (1 1 1) heterojunctions

Methods of vacuum evaporation have been developed which make it possible to grow epitaxial films of II–VI compounds with defect densities comparable with those in the best hetero-epitaxial films of other materials. Determinations of the epitaxial orientation relationship between II–VI films and substrates have been made for many substrate materials and for the three singular substrate orientations (1 0 0), (1 1 0) and (1 1 1). Prior to the present work these orientation relationships all corresponded to parallel alignment and symmetry matching. This could be understood as these relationships ensure the possibility of high coincidence site density interface structures which minimize the interfacial energy. The evidence for these generalizations was reviewed previously [1].

This paper is concerned with the epitaxial orientation relation between CdSe films and (1 1 1) Ge substrates, which was briefly reported in an earlier paper [2], and with a possible explanation for this orientation relation.

The films were grown by focused electron beam evaporation in a vacuum of a few times 10^{-6} Torr, as previously described [2]. With this technique, to obtain continuous films of II–VI compounds including CdSe, thicknesses of about 0.2 μm (2000 Å) must be grown. At these thicknesses transmission electron micrographic contrast is poor and the area density of defects is too high for individual dislocations to be analysed. It was, therefore, necessary to thin the CdSe films after growth in a uniform manner before locally jet-thinning the Ge substrates as in [2] in order to attempt to observe the misfit dislocations in the CdSe/Ge heterojunction interfaces. The films were

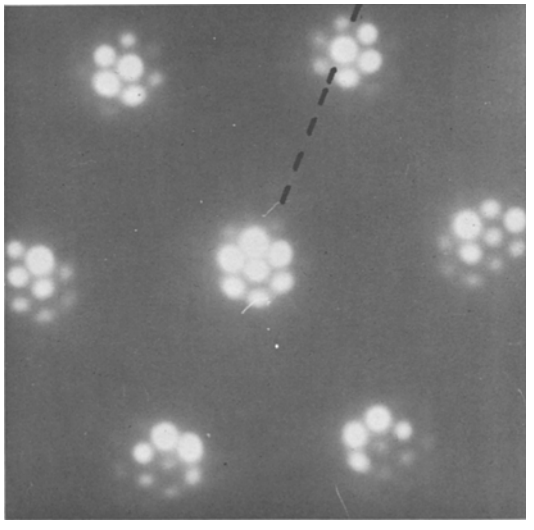

Figure 1 Transmission electron diffraction pattern from an area of equal thicknesses of CdSe and Ge.

thinned by immersion for 8 sec at room temperature in a polishing solution made by adding potassium permanganate to concentrated sulphuric acid until the liquid turned dark green [3]. The doubly thinned specimens were examined in a Philips EM301 transmission electron microscope with results that were inconclusive but suggestive, as will be reported below.

The epitaxial orientation relationship is defined by the Moiré diffraction patterns that are observed in areas of the specimen where equal thicknesses of the two semiconductors are present, as shown in Fig. 1. The interpretation of such patterns for parallel alignment is shown in Fig. 2. This is the plot of the pattern due to a film with the sphalerite structure grown on a (1 1 1) surface of a substrate with the diamond structure, as has been found for a number of combinations of II–VI compounds and Ge [1]. This is the pattern for the epitaxial orientation relationship (1 1 1) II–VI parallel to (1 1 1) Ge with [1 1 0] II–VI exactly parallel to [1 1 0] Ge [4]. For clarity attention will now be confined to the Moiré rosette of spots around the $0\bar{2}2$ CdSe spot alone. The array for exactly parallel alignment (as in Fig. 2) is shown again in Fig. 3a for comparison with the array actually found for the case of CdSe on Ge as shown in Fig. 1 and plotted in Fig. 3b. The rosette of spots in the present case is rotated about the $0\bar{2}2$ CdSe spot by about 30° from its position for exact parallelism. By considering the reciprocal lattic vectors to neighbouring CdSe and Ge spots, as shown in Fig. 4, it is found that

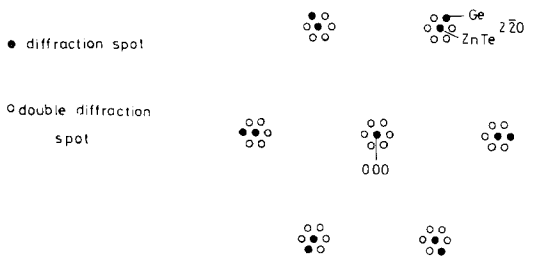

Figure 2 Plot of the Moiré diffraction pattern of overlapping Ge in (1 1 1) orientation and a sphalerite structure film in parallel alignment with the substrate. Such patterns are obtained in the case of ZnTe grown on (1 1 1) Ge [4].

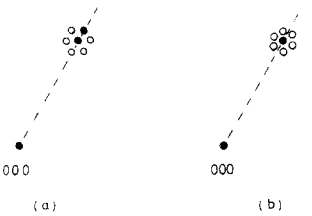

Figure 3 Plots of portions of the Moiré diffraction patterns for II–VI films epitaxially grown on (1 1 1) Ge for the cases of (a) exactly parallel alignment and (b) azimuthal rotation from parallel alignment as seen in Fig 1.

$$\tan\theta = \frac{|g_{rot}|}{|g_{diff}|} \qquad (1)$$

where g_{rot} is the vector representing the azimuthal rotation from parallel alignment and g_{diff} is the difference between the $0\bar{2}2$ vectors in CdSe and in Ge. This can be rewritten as

$$\frac{\sin\alpha}{d_1} = |g_{diff}|\tan\theta \qquad (2)$$

i.e.

$$\sin\alpha = \left(\frac{d_1 - d_2}{d_2}\right)\tan\theta \qquad (3)$$

where d_1 and d_2 are the $0\bar{2}2$ plane spacings in Ge and in CdSe respectively and θ, defined in Fig 4, can be seen in Fig. 1 to be approximately 30°. (The Moiré rosettes are rotated to a position of symmetry about the $0\bar{2}2$ CdSe g vector). Substi-

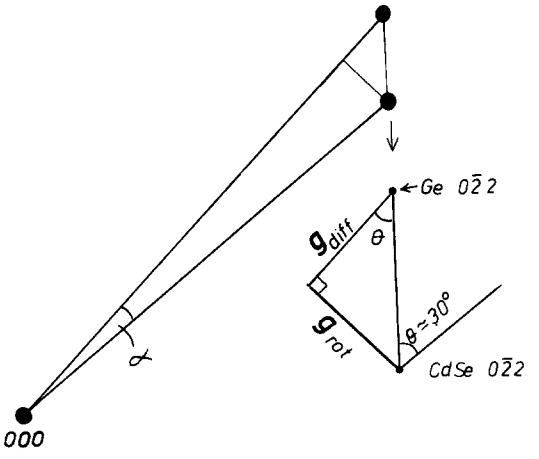

Figure 4 Reciprocal lattice vectors for the azimuthally rotated case, for neighbouring Ge and CdSe spots as in Fig. 3b $\mathbf{g}_{diff}$ is the difference between these two vectors and $\mathbf{g}_{rot}$ represents the azimuthal rotation. α is the angular misorientation across the interface (after Gejji and Holt [2]).

tuting the values of d_1 and d_2 gives $\alpha = 2°24'$ (± about 30′). When this azimuthal rotation was first noticed it was found that it did not have any simple crystallographic interpretation but it was suggested that it might perhaps be understood in terms of the incorporation of screw-type misfit dislocations in the interface [2].

The special interest of the misfit dislocations in CdSe/Ge (1 1 1) heterojunctions in relation to the unexpected nearly-parallel, aximuthally rotated orientation relationship, in addition to their interest in relation to the electrical properties of the heterojunction [5, 6], motivated the attempt to thin the specimens from each side in turn as described above. The result was that in a few small areas it was possible to obtain micrographs which showed what might be misfit dislocations. This interpretation of the dark lines in question was based on two factors. These were their broader, darker, network-form appearance and their spacing. They were found to have twice the spacing of the narrower light, straight 2 2 0 Moiré fringes which were readily visible over large areas, unlike the possible misfit dislocations. For Moiré fringes to have this doubled 5.6 ± 0.6 nm (56 Å) spacing they would have to arise from interference between the undeviated 0 0 0 beam and a beam that had undergone 1 1 0 reflections in both the CdSe and the Ge. But 1 1 0 reflections are forbidden in both the sphalerite structure of CdSe and the diamond structure of Ge by structure factor considerations and do not occur in the observed diffraction patterns. The other most significant feature of these lines which appear to be misfit dislocations is that they run in ⟨1 1 0⟩ directions and not the ⟨1 1 2⟩ directions expected [6] for pure edge misfit dislocations with ⟨1 1 0⟩ Burgers vectors lying in the (1 1 1) interface plane for the case of parallel alignment.

Unfortunately, owing to these lines only being visible in small areas and over narrow ranges of specimen tilt in the microscope, it has not been possible to carry out a Burgers vector determination on these possible misfit dislocations and none of our micrographs therefore really merit publication.

These observations did, however, strongly suggest that it would be worthwhile considering the effect of networks of misfit dislocations that are not of the edge type. There are two geometrical possibilities if the dislocations have ⟨1 1 0⟩ Burgers vectors in the (1 1 1) plane and ⟨1 1 0⟩ line directions also in this plane. The misfit dislocations may then be either 60° dislocations or screw dislocations [7, 8]. A network of screw dislocations would constitute a twist boundary and might account for the observed azimuthal rotation, but could not help to accommodate the lattice parameters misfit. The 60° dislocations with both edge and screw components could assist in accommodating both types of "misfit".

It, therefore, seemed worthwhile to examine quantitatively the consequences of the hypothesis that the CdSe/Ge (1 1 1) interface contains a network of 60° misfit dislocations with their Burgers vectors in the interface and the result of this analysis [9] is presented below.

No theory is available to treat the elastic energy of an azimuthally rotated, nearly parallel interface of the type found here (Fig. 1), in which both dilatational and shear (rotational) misfit occurs across the interface. However, an heuristic argument, which follows, shows that a crystallographically self-consistent account can be given which is in agreement with all the facts observed thus far.

The 60° dislocations of an hypothetical misfit dislocation network have edge components with Burgers vectors $\mathbf{b}_e = \mathbf{b} \sin 60°$ and screw com-

ponents with Burgers vectors $\mathbf{b}_s = \mathbf{b} \cos 60°$. The standard Brooks formula [10] for the spacing of edge dislocations, p_e, in a parallel alignment lattice parameter-misfit interface is

$$p_e = \frac{b}{\delta} = \frac{(d_1 + d_2)/2}{2(d_1 - d_2)/(d_1 + d_2)} \quad (4)$$

where b is the Burgers vector of the misfit dislocations, δ is the misfit and d_1 and d_2 are the interatomic repeat distances in materials 1 and 2, which are parallel to b. This can be rewritten as

$$p_e = \frac{d_1 + d_2}{2} \frac{b}{d_1 - d_2} \quad (5)$$

That is, it is equal to the product of the average repeat distance times the number of difference units to make up the Burgers vector. It is now clear how this must be modified to apply to the present "nearly-parallel, azimuthally rotated" interface. All three distances must be resolved along the same direction. Choosing this to be the ⟨1 1 0⟩ direction in the CdSe, the material with the larger lattice parameter, d_1 and d_2 are obtained as

$$d_1 = a_{CdSe}/\sqrt{2}\, d_2 = (a_{Ge}/\sqrt{2}) \cos 2°24' \quad (6)$$

and

$$b_e = b \sin 60° = (a/\sqrt{2}) \sin 60° \quad (7)$$

There are three possible values for "a" in Equation 7. If the misfit dislocations occur in the CdSe, in the Ge or in the interface then the appropriate value of a would be a_{CdSe}, a_{Ge} or $(a_{CdSe} + a_{Ge})/2$ respectively. Since the CdSe film is thin and grown on a massive Ge substrate it is likely that the appropriate value is $a \simeq a_{CdSe}$.

The two lattice parameters are given by the ASTM Powder Data file as $a_{CdSe} = 6.077$ Å and $a_{Ge} = 5.6576$ Å. Substituting these values into Equations 6 and 7, and these expressions into Equation 5 gives $p_e = 5.2$ mm (52 Å) in agreement with the "observed" spacing for the dark lines mentioned above.

Now let it be assumed that the standard expression for the spacing of screw dislocations in a twist boundary [11] applies to the screw components in the 60° misfit dislocation network, i.e.

$$p_s = \frac{b_s}{2 \sin \alpha/2} \quad (8)$$

where α is the azimuthal rotation angle. Setting the spacing for the screw components equal to the previously calculated spacing i.e. $p_s = p_e = 5.2$ nm the azimuthal rotation that would be produced by the 60° misfit dislocations is obtained once b_s is determined. As discussed in the previous calculation there are three possibilities and again we assume that the value of b_s is that for dislocations in the CdSe. This value substituted into Equation 8 gives $\alpha = 2°22'$ in good agreement with the experimental value of $2°24'$ (± 30′, allowing generously for the uncertainty in the value of θ in Equation 3 found above). The more probable CdSe Burgers vector case again fits best.

These calculations have shown that the hypothesis that a 60° misfit dislocation network occurs in the CdSe/Ge (1 1 1) heterojunction interface can account for the lattice parameter misfit if this is all taken up by the edge components and the dislocation spacing is about 5.2 nm. Moreover, the azimuthal rotation produced by the screw components is then in agreement with the observed value, assuming the misfit dislocations to occur in the film.

Some transmission electron microscope observations of an inconclusive kind were also consistent with the hypothesis that what was seen were 60° dislocations in a network with a 5.6 nm spacing.

At present it has not been proved that 60° misfit dislocations do occur nor that a 60° misfit dislocation network i.e. a nearly-parallel, azimuthally rotated interface, is of lower energy than any alternative and, in particular, than an edge-dislocation misfit network, i.e. a parallel alignment interface. Thus what has been demonstrated is just that the 60° misfit dislocation network hypothesis can account self-consistently for both the change of lattice parameter and the azimuthal rotation across the CdSe/Ge (1 1 1) interface and that there is some experimental support for the idea.

Some evidence for screw dislocation misfit networks and accompanying rotational misalignment was recently reported by Matthews [12] and the possibility of other than edge misfit dislocations has been discussed in terms of the theory of continuous distributions of surface dislocations [13]. Igarashi [14] observed small angular deviations from parallel alignment of the c-axis, in hexagonal (wurtzite) structure CdS epitaxial films,

with a ⟨1 1 1⟩ axis in several cubic system substrates. He showed that those deviations could be accounted for quantitatively by a simple misfit dislocation model. Thus, it is clear that small deviations from parallel epitaxial alignment occur in a number of cases and it appears generally that these phenomena can be understood in misfit dislocation terms.

Acknowledgements

Thanks are due to Professor J.G. Ball for the provision of research facilities. One of us (FHG) wishes to thank the Governments of India and of Kamataka State for the provision of a study grant.

References

1. D. B. HOLT, *Thin Solid Films* **24** (1974) 1.
2. F. H. GEJJI and D. B. HOLT, *J. Electrochem. Soc.* **122** (1975) 535.
3. J. E. ROWE and R. A. FORMAN, *J. Appl. Phys.* **39** (1968) 1917.
4. A. R. MUFTI and D. B. HOLT, *J. Mater. Sci.* 7 (1972) 694.
5. W. G. OLDHAM and A. G. MILNES, *Solid State Electron.* 7 (1964) 153.
6. D. B. HOLT, *J. Phys. Chem. Solids* **27** (1966) 1053.
7. J. HORNSTRA, *ibid.* **5** (1958) 129.
8. D. B. HOLT, *ibid.* **23** (1962) 1353.
9. F. H. GEJJI, Ph. D. Thesis, University of London (1976).
10. H. BROOKS, "Metal Interfaces" (American Society of Metals, Cleveland, 1952) pp. 20–64.
11. W. T. READ "Dislocations in Crystals" (McGraw–Hill, New York, 1953) p. 178.
12. J. W. MATTHEWS, *Phil. Mag.* **29** (1974) 797.
13. C. M. SARGENT and G. R. PURDEY, *ibid.* **32** (1975) 27.
14. O. IGARASHI, *J. Appl. Phys.* **42** (1971) 4035.

Received 9 December 1977
and accepted 2 February 1978.

F. H. GEJJI*
D. B. HOLT
Department of Metallurgy and Materials Science, Imperial College of Science and Technology, London, UK

*Present address: Government Polytechnic, Bijapur, Kamataka State, India.

Strain-induced continuous recrystallization in Zr-bearing aluminium alloys

It has recently been demonstrated that a series of aluminium alloys can be made superplastic by the addition of about 0.5% Zr [1–4]. Although superplastic elongation requires a stable fine-grained structure, a salient structural aspect regarding these alloys is that, prior to superplastic deformation, they generally are not recrystallized. A fine-grained structure is obtained during hot forming after an initial 10 to 50% straining, apparently due to a continuous recrystallization process [3]. The stability of the as recrystallized structure during continued plastic flow relies on the inhibition of grain growth by finely-dispersed Al_3Zr-particles. The mechanism, however, by which the fine-grained structure is obtained cannot be considered as established.

This note reports some preliminary results on the structural stability of a Zr-bearing Al–Mn alloy (Al–0.9 Mn–0.4 Zr) during hot deformation using strain rates typical of superplastic forming operations. The alloy, which was of commercial purity, was chill cast. Following casting the alloy was cold rolled about 85% and then given a pre-treatment of 4 h at 440° C which produced a subgrain structure stabilized by Zr- and MnFeSi-rich particles. Fig. 1 illustrates the fine dispersion of the metastable cubic Al_3Zr particles. The distribution of the MnFeSi-rich dispersoids is similar to that reported in [5]. The stability of this structure has been followed during isothermal annealing at 500° C and during plastic straining at 480° C. The tensile specimens had a gauge length of about 10 mm, a width of 5.5 mm and thickness about 1 mm. The specimens were deformed at a constant velocity of 0.2 cm min^{-1}, i.e. at an initial strain rate of 3.3×10^{-3} sec^{-1}.

The pre-heat treated alloy has been annealed for several hours at 500° C without any signs of recrystallization. During such heat treatments only minor subgrain growth occurred. During hot deformation, however, the subgrain size was found to increase with increasing strain as illustrated by the diagram in Fig. 2. The TEM micrographs in Figs. 3a, b and c show the undeformed subgrain structure, and those after 40% and 180% deformation, respectively.